Hindawi
Mathematical Problems in Engineering
Volume 2019, Article ID 2085962, 18 pages
https://doi.org/10.1155/2019/2085962

Research Article

Optimization of Scanning Parameters in Coordinate Metrology Using Grey Relational Analysis and Fuzzy Logic

Syed Hammad Mian, Usama Umer, and Hisham Alkhalefah

Advanced Manufacturing Institute, King Saud University, Riyadh 11421, Saudi Arabia

Correspondence should be addressed to Syed Hammad Mian; smien@ksu.edu.sa

Received 5 January 2019; Revised 5 June 2019; Accepted 12 June 2019; Published 3 July 2019

Academic Editor: Alessandro Gasparetto

The phenomenon of coordinate measuring machines has led to a significant improvement in accuracy, adaptability, and reliability for measurement jobs. The coordinate measuring machines with scanning capabilities provide the alternative to output precise acquisition at a faster rate. However, they are less accurate as compared to discrete probing systems and slower than the noncontact techniques. Therefore, the data acquisition using a scanning touch probe needs improvement, so that it can provide commendable performance both in terms of accuracy and scanning time. The determination of appropriate scanning parameters is crucial to minimize the inaccuracy and time associated with the scanning process. However, it can be demanding as well as unreliable owing to the presence of uncertainty from a multitude of factors that may influence the measurement process. The optimization of data acquisition using a scanning touch probe is a multiresponse process which involves definite uncertainties from various sources. Therefore, multioptimization tools based on grey relational analysis coupled with principal component analysis and fuzzy logic were employed to enhance the utilization of the scanning touch probe. The work described here has the objective to identify the appropriate combination of scanning factors which can simultaneously boost the accuracy and lessen the scanning time. This study demonstrates the capability and effectiveness of the uncertainty theory based optimization methods in coordinate metrology. It also suggests that the uncertainty associated with the parameter optimization can be significantly reduced using these techniques. It has also been noticed that the results from the two techniques are in accord, which corroborates their application in coordinate metrology. The result from this study can be applied to other probing systems and can be broadened to include more experiments and parameters in various scenarios as needed by the specific application.

1. Introduction

In recent years, the metrology function has transformed into an indispensable component of manufacturing industries. It can be attributed to strict accuracy requirements as well as the volatile customer demands. Currently, the most commonly used approach for inspection is coordinate measuring machines (CMMs), owing to their excellent performance in terms of accuracy and precision. Indeed, the CMMs can be sighted in every industry, including automotive, aerospace, and medical. It is a complicated system, where its various constituting elements exhibit variable performance, thus affecting measurement results. There is always an element of uncertainty or vagueness that results in the discrepancy between the measured result and the true value. According to Wilhelm et al. [1] and Takamasu [2], a number of factors, namely, probing system, evaluation software, number and distribution of points, temperature, etc., may contribute to uncertainty, thus affecting the measurement results.

The inspection process using CMM involves the acquisition of point coordinates to ascertain whether the measuring feature is within the specified limit or not. This procedure of data acquisition is known as digitization or scanning. There are several digitization techniques, such as a touch trigger probe, scanning touch probe, and laser scanning, which can be employed to gather point's coordinates on the measurand [3, 4]. As the different approaches possess variable performance and characteristics, therefore, it is important to select the technique appropriate for a given application. Indeed, the selection and their effective utilization depend on the understanding of the application and the chosen

operating conditions. For instance, scanning touch probe can be considered as the suitable alternative for the digitization of free form or sculptured surfaces. It is because the scanning touch probe, which works in continuous contact mode provide higher accuracy and precision in comparison to noncontact data acquisition systems. Moreover, their ability to gather data without having to back off from the surface results in faster measurements in contrast to touch trigger probes [5]. However, the fundamental issue with these probes is that they are neither as accurate as touch trigger probes nor as efficient as noncontact systems. Therefore, a trade-off between accuracy and speed must be accomplished through the pursuit of well-suited operation settings. It suggests that the superlative operation of the scanning touch probe can be achieved through the appropriate selection of scanning parameters.

There have been many instances, where different scanning parameters were analyzed to enhance the quality of measurement using CMM. For example, Feng and Pandey [6] developed an approach based on fractional factorial and analysis of variance (ANOVA) to study the influence of digitization parameters. They established empirical models depending on the relationship between digitizing accuracy and various factors to help in the selection of digitization parameters. The digitization factors comprising travel speeds, pitch, probe angles (part orientations), probe sizes, and feature sizes were investigated to quantify their effect on digitization accuracy. Similarly, factorial design and statistical ANOVA were applied by Piratelli-Filho and DiGiacomo [7] to study the impact of length, position, and orientation of test specimen on CMM measurement errors. Furthermore, the influence of factors, including speed, stylus length, probe ratio, measured points, starting position (offset), was investigated by Feng et al. [8], to assess the CMM performance. They also employed fractional factorial and ANOVA in their study. To determine important scanning parameters, Korosec et al. [9] modeled contactless scanning process using response surface methodology. The techniques based on neural network and ANOVA were employed to predict response, based on the combination of input parameters. Lately, Pathak and Singh, [10] developed a prediction model to measure the influence of scanning angle and distance of the laser beam from the part surface using response surface methodology and ANOVA. They further optimized the parameters using modified particle swarm optimization algorithm for improved digitization accuracy.

It has been realized through previous works that the attainment of superior performance in CMM inspection is a formidable exercise. The choice of scanning parameters, their range, and the optimal solution is demanding owing to the interaction among various parameters as well as the existence of uncertain information in the CMM system. The task becomes even more complicated due to the existence of multiple responses and the requirement of their concurrent control within an accepted range. Notice that each scanning parameter exhibits a variable and a conflicting consequence on each response. It advocates the need of an optimization tool which can consider imprecise information in order to determine the appropriate blend of scanning parameters. Although numerous efforts have investigated the CMM scanning parameters, but none of them have utilized approaches based on uncertainty assumptions or grey theory, such as grey relational analysis (GRA), GRA coupled with principal component analysis (GRA-PCA), and fuzzy logic.

The unparalleled potential of GRA-PCA and fuzzy logic can be established through plentiful studies in the optimization of machining processes. For example, the theory of GRA was used by Tosun [11] to acquire the most appropriate combination of drilling process parameters. Their objective was the minimization of surface roughness and the burr height through optimized drilling parameters. Similarly, Siddiquee et al. [12] described the successful utilization of GRA in the optimization of process parameters in friction stir welding of Aluminum alloy with multiple responses. They asserted the benefits of GRA in terms of simplicity and ease of application in the optimum design of any process with multiple-performance characteristics. Indeed, the GRA and fuzzy logic have been implemented to solve a variety of optimization problems, such as optimization of drilling parameters in B_4C reinforced metal matrix composites (MMCs) (Taskesen and Kütükde [13]), identification of optimal cutting parameters in high-speed end milling (Lu et al. [14]), investigation of the machinability in turning process (Sehgal and Meenu [15]; Tzeng et al. [16]; Ramanujam et al. [17]), multiresponse optimization of mechanical properties in self-healing glass fiber reinforced plastic (Mercy et al. [18]), optimization of electric discharge machining process (Lin et al. [19]), parameter optimization in grinding (Liu et al. [20]), and acquisition of suitable laser welding parameters (Maheswaran et al. [21]). These investigations in machining have demonstrated GRA-PCA and fuzzy logic as powerful mathematical tools to analyze any process with multiple-performance characteristics. These techniques are proficient in quantifying the uncertainty of information and the vagueness of measurement, and they can handle innumerable factors and responses. They are also useful in carrying out prediction, relational analysis, and decision making in numerous fields.

The optimization of data acquisition using a scanning touch probe is a multiresponse process with the existence of significant imprecision from different sources, namely, the environment, metrologists, equipment, etc. A systematic experimental investigation and analysis are imperative in such situations or scenarios which involve multiple parameters, several responses, and eventually process improvement [22–24]. Since the work presented here has the objective of enhancing the performance of a CMM mounted with scanning or analog probe head, a methodical experimental approach and multioptimization tools based on GRA-PCA and fuzzy logic were applied to figure out the best combination of scanning parameters and optimize the performance of the scanning touch probe. The structure of the paper is organized in the following manner. The methodology has been discussed in detail in the subsequent section. Then, the optimization results have been analyzed followed by the conclusion which summarizes the work and its results.

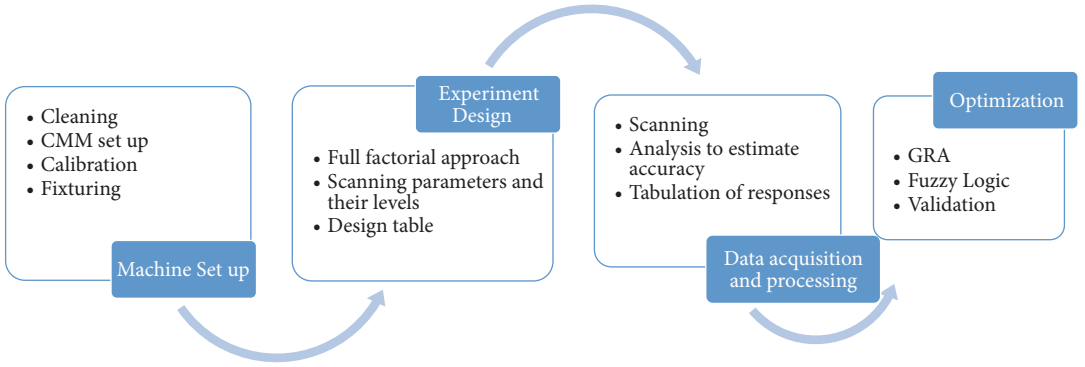

Figure 1: Adopted methodology.

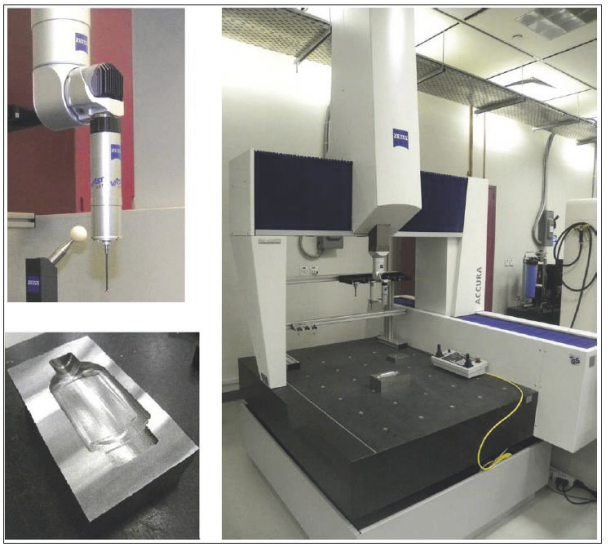

Figure 2: Experimental setup.

2. Methodology

The competence of scanning touch probe to gather points precisely makes them the initial choice for inspecting and reverse engineering any surface. A simple test procedure was adopted to determine the scanning parameters that lead to higher accuracy in lesser scanning time. The flow diagram depicting the developed methodology can be seen in Figure 1.

2.1. Machine Setup. The test specimen was digitized using a scanning touch probe mounted on bridge type CMM as shown in Figure 2. A medium-sized CMM employed in this investigation had an accuracy of (1.6 + L/333) μm, which complies with DIN EN ISO 10360-2:2001. The contact probe used in this investigation had a tip radius of 1.5 mm and tip length of 60 mm.

The cleaning of test part, probing system, and guideways for any dust particle was indispensable in order to minimize measurement uncertainty and gather accurate point coordinates. Subsequent to cleaning, the CMM was set up by mounting the probing system, switching on the drives and pressure supply, etc. Then, the part was placed and fixed appropriately on the machine table in such a way that the measurement error could be minimized. Prior to conducting actual experiments, the scanning touch probe was calibrated. The temperature and humidity measured during the experiment were 22°C and 8%, respectively.

2.2. Experiment Design. The experiments for this work were planned using full factorial design (FFD) approach in Minitab 18 statistical software. The FFD technique was chosen because it employs all possible combinations of levels of different factors and provides precise results without losing any information [25–27]. It provides users with a rational and a competent method for identifying optimum parameters for a production process.

The fundamental step in the implementation of FFD was the selection of critical scanning parameters, which influence the data acquisition process. From the experience, machine manual, and pilot study, the scanning parameters, namely, scanning speed, distance between points, and the distance between lines were chosen [28]. The scanning speed represents the distance travelled by the probe per second and is measured in mm/s. The distance between points defines

Table 1: Scanning parameters and their levels.

Scanning parameters	Units	Levels		
		Level 1	Level 2	Level 3
Scanning speed	mm/s	5	7	10
Distance between points	mm	0.0025	0.005	0.01
Distance between lines	mm	0.3	0.5	0.7

the distance between points on each scan line, whereas the distance between lines characterizes the distance between scan lines. These two parameters are measured in mm. The selected parameters and their levels are presented in Table 1. Since contact probes require larger scanning time, it was very important to achieve higher accuracy in lesser scanning time. As a consequence, the output responses utilized to assess the scanning performance were scanning time and accuracy.

The experiments were conducted according to FFD three-level design (3^3). A total of 27 experiments were executed according to the design scheme as shown in Table 2.

2.3. Data Acquisition and Processing. The scanning (or the experiments) was carried out at different combinations of scanning parameters. As a result, the different point cloud sets as depicted in Figure 3 were acquired at different combinations. The scanning time was recorded from the time; the probe contacted the first point until it captured the last point. In order to estimate the accuracy, the point cloud data were transformed into Computer Aided Design (CAD) models and analyzed in the analysis software.

The accuracy was quantified through the Root Mean Square (RMS) value, which was computed by the deviations observed between a number of individual predefined points on actual part and corresponding points in the CAD model [28]. The RMS value provided an indication of the overall accuracy of the CAD model. The approach adopted to calculate the RMS has been described in Figure 4.

The CAD models were saved in Initial Graphics Exchange Specification (IGES) format and imported in the analysis software. Consequently, it was aligned with the actual part in order to place it in the same coordinate system as that of the actual part and the same zero point was defined for both of them. Then, the safety cube was established by setting appropriate values for clearance plane, back away path, etc. Finally, a number of points were identified at various locations in the CAD model and these points were probed by the touch trigger probe to obtain deviations. These points were then used to estimate the RMS value for that particular CAD model. The deviations at various individual points of the CAD model obtained using experimental run 1 can be realized in Figure 5.

After the execution of all experiments, the estimated output responses, namely scanning time (minutes) and RMS (μm) were tabulated as shown in Table 3. This tabulated information was subsequently utilized for optimization of scanning parameters using GRA-PCA and fuzzy logic.

2.4. Optimization. During the optimization of process parameters, the experimenter gathers as much information as possible about the important factors and uncertainty contributors through preliminary experiments, literature survey, etc. However, it is cumbersome and most often impossible to acquire all the details about the process, which means that the decision is generally taken in fuzzy, i.e., in the presence of imprecise information. It is where fuzzy logic and GRA find their application. Therefore, in this research, the optimization has been achieved with the aid of GRA-PCA and fuzzy logic. These techniques are adequate to consider the uncertainty and vagueness associated with coordinate metrology and provide precise results. The different steps of these techniques have been described below.

2.4.1. Grey Relational Analysis. The GRA can be defined as a multistep procedure to optimize uncertain systems and fragmentary problems. It is typically utilized for determining the process parameters and measuring the correlation between multiresponses [29]. The concept of grey theory was first proposed by Prof. Deng from the grey set in combination with systems theory, theory of space, and control theory [30].

The remarkable characteristics about grey theory are its capability to overcome the inconclusiveness and confusion of human decisions through mathematical protocol or language. The GRA exhibits numerous benefits, including satisfactory results with lesser data and computational simplicity, [31, 32]. It is especially useful when the experiments cannot be performed precisely and it aids to compensate the limitations in statistical regression [33]. The GRA can successfully be combined with other methods, such as PCA to enhance the quality of decision making [34]. In this study, the corresponding weighting values for GRA were obtained from the PCA.

The PCA was first introduced by Pearson in 1901 [35] and developed into a statistical tool by Hoteling [36]. It aids to simplify the problem by transforming many correlated variables into lesser uncorrelated and independent principal components and maintain the initial information as much as possible through linear combination. The main benefit of PCA is that it compresses the data by minimizing the number of dimensions without sacrificing significant information. It can be utilized to emphasize variation and bring out strong patterns in a dataset. Indeed, it is most often used to make data easy to explore and visualize. The implementation of GRA-PCA comprised five primary steps [37]: generation of grey relational, definition of the reference sequence, calculation of grey relational coefficients, computation of weights using PCA, and finally the estimation of grey relational grade.

Step 1. The grey relational generating step involved the translation of given responses into comparability sequences

Table 2: Scheme to conduct the experiments.

Experiment run	Scanning speed	Distance between points	Distance between lines
1	5	0.005	0.5
2	5	0.005	0.7
3	10	0.0025	0.3
4	7	0.0025	0.3
5	7	0.005	0.7
6	10	0.0025	0.7
7	10	0.005	0.3
8	10	0.01	0.5
9	5	0.0025	0.7
10	10	0.005	0.7
11	7	0.01	0.3
12	7	0.01	0.5
13	7	0.005	0.5
14	7	0.005	0.3
15	10	0.01	0.7
16	10	0.0025	0.5
17	5	0.005	0.3
18	5	0.01	0.7
19	5	0.0025	0.5
20	7	0.0025	0.5
21	5	0.01	0.5
22	5	0.01	0.3
23	7	0.0025	0.7
24	7	0.01	0.7
25	5	0.0025	0.3
26	10	0.005	0.5
27	10	0.01	0.3

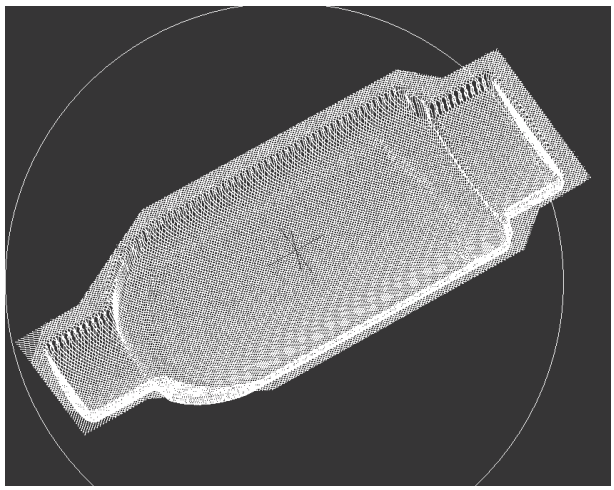

Figure 3: Acquired point cloud.

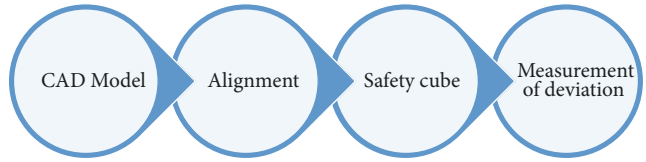

Figure 4: Procedure to estimate RMS.

Table 3: Measured responses at different runs.

Experiment Run	Scanning time	RMS	Experiment Run	Scanning time	RMS	Experiment Run	Scanning time	RMS
1	270.96	21	10	162.35	33	19	317.66	21
2	207.86	23	11	389.80	24	20	289.76	21
3	362.77	25	12	253.03	21	21	265.84	22
4	404.62	19	13	261.82	22	22	417.70	21
5	169.96	23	14	400.53	23	23	174.47	21
6	168.05	35	15	153.23	30	24	160.08	27
7	357.83	25	16	213.56	38	25	471.98	15
8	203.09	31	17	427.58	17	26	212.97	36
9	212.80	20	18	203.40	25	27	356.84	26

[14]. The utilized linear data preprocessing method can be expressed as follows.

The-larger-the-better (the higher the response value, the better)

$$x_i^*(k) = \frac{x_i^{(O)}(k) - \min x_i^{(O)}(k)}{\max x_i^{(O)}(k) - \min x_i^{(O)}(k)} \quad (1)$$

The-smaller-the-better (the lower the response value, the better)

$$x_i^*(k) = \frac{\max x_i^{(O)}(k) - x_i^{(O)}(k)}{\max x_i^{(O)}(k) - \min x_i^{(O)}(k)} \quad (2)$$

The-nominal-the-better characteristic (set the response as target value (TV))

$$x_i^*(k) = \frac{\left|x_i^{(O)}(k) - TV\right|}{\max\left\{\max x_i^{(O)}(k) - TV, TV - \min x_i^{(O)}(k)\right\}} \quad (3)$$

where $x_i^*(k)$ is the sequence after the data processing; $x_i^{(O)}(k)$ is the original sequence of responses, where $i = 1, 2, \ldots, m$ and $k = 1, 2, \ldots, n$; $\max x_i^{(O)}(k)$ is the largest value of $x_i^{(O)}(k)$; $\min x_i^{(O)}(k)$ is the smallest value of $x_i^{(O)}(k)$. Moreover, m represents the number of responses and n represents the number of experiment runs.

Step 2. Depending on these comparability sequences, a reference sequence (ideal target sequence) was determined. It was obtained by taking the maximum value in the comparability sequence of the corresponding response.

Step 3. Subsequently, the grey relational coefficients (GRCs) were calculated using the preprocessed sequences. The GRCs were estimated as follows:

$$GRC\left(x_O^*(k), x_i^*(k)\right) = \frac{\Delta_{min} + \varepsilon\Delta_{max}}{\Delta_{oi}(k) + \epsilon\Delta_{max}} \quad (4)$$

where $\Delta_{oi}(k)$ is the deviation sequence of the reference sequence $x_O{}^*(k)$ and the comparability $x_i{}^*(k)$, i.e., $\Delta_{oi}(k) = |x_O{}^*(k) - x_i{}^*(k)|$ is the absolute value of the difference between $x_O{}^*(k)$ and $x_i{}^*(k)$.

$$\Delta_{min} = \min_{\forall i} \min_{\forall k} \Delta_{\mathrm{oi}}(k)$$
$$and\ \Delta_{max} = \max_{\forall i} \max_{\forall k} \Delta_{\mathrm{oi}}(k) \quad (5)$$

ϵ: distinguishing coefficient, ϵ [0, 1]. Generally, ϵ is set as 0.5. The purpose of defining this coefficient is to show the relational degree between the reference sequences $x_O^*(k)$ and comparability sequences $x_i^*(k)$, where $i = 1, 2, \ldots, m$ and $k = 1, 2, \ldots, n$.

Step 4. In order to compute the weights for the responses, the PCA was performed. The computation in PCA consisted of the determination of the correlation coefficient array (CCA), followed by the calculation of eigenvalues and eigenvectors and, finally, the computation of uncorrelated principal components. The following set of equations were utilized to obtain the principal components.

$$\text{Correlation Coefficient Array, } CCA_{uv} = \left(\frac{\mathrm{cov}\left(x_i(u), x_i(v)\right)}{\sigma_i(u) * \sigma_i(v)}\right) \quad (6)$$

where $\mathrm{cov}(x_i(u), x_i(v)$ is the covariance of sequences $x_i(u)$ and $x_i(v)$, $\sigma_i(u)$ is the standard deviation of sequence $x_i(u)$; $\sigma_i(v)$ is the standard deviation of sequence $x_i(v)$.

The eigenvalues and eigenvectors were obtained using the following formulation:

$$\left(CCA - \lambda_k I_m\right) E_{ik} = 0 \quad (7)$$

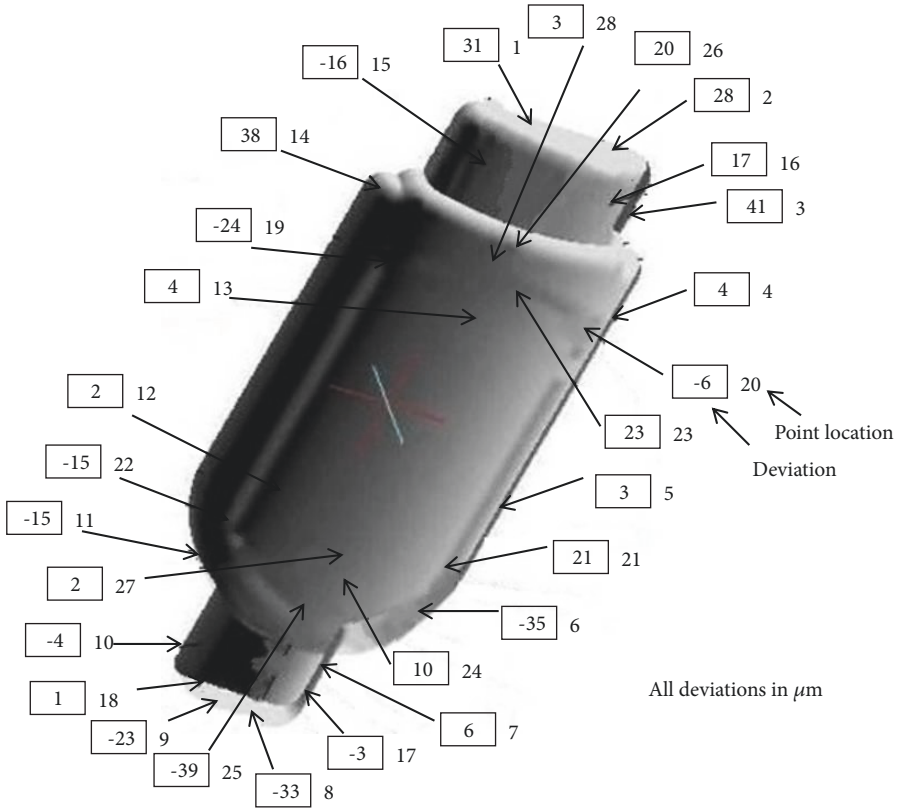

Figure 5: Deviations at individual points (Experimental Run 1).

λ_k represents eigenvalues and E_{ik} represent the eigenvectors corresponding to the eigenvalues. The principal components can be estimated as follows:

$$P_{mk} = \sum_{i=1}^{n} x_m(i) \,.\, E_{ik} \tag{8}$$

where P_{mk} is called the kth principal component. The principal components have to be arranged in decreasing order with respect to the variance, which suggest that the first principal component causes most variation in the data. The formulation in (8) can be utilized to estimate the first principal component through the summation of the products of the *GRC* of the two responses multiplied by the elements of the eigenvector, which corresponded to the largest eigenvalue.

Step 5. Finally, the grey relational grade (*GRG*) was estimated. The *GRG* is a weighting-sum of the *GRC* and it is defined as follows.

$$GRG\left(x_o*, x_i^*\right) = \sum_{k=1}^{n} \beta_k \gamma\left(x_o*(k), x_i^*(k)\right) \tag{9}$$

where β_k represents the weighting value of the kth performance characteristic, and $\sum_{k=1}^{n} \beta_k = 1$. The *GRG* ($x_o*$, x_i^*) represents the level of correlation between the reference sequence and the comparability sequence. If the two sequences are identically coincidence, then the value of *GRG* is equal to 1. If a particular comparability sequence is more important than the other comparability sequences to the reference sequence, then the *GRG* for that comparability sequence will be higher than other *GRG*.

2.4.2. Fuzzy Logic. The results acquired using GRA-PCA were further confirmed using the fuzzy logic. It can be described as the mathematical model which is based on fuzzy set theory. It was initially introduced by Zadeh [38] in order to deal with uncertainty. The fuzzy system can be identified as a computer program to translate multiple inputs into single output using fuzzy set theory, fuzzy IF-THEN-rules and fuzzy reasoning [33, 39]. It comprises a fuzzifier, an inference engine and defuzzifier as shown in Figure 6. The fuzzifier converts the crisp input to a linguistic variable using the membership functions, the inference engine converts fuzzy input to the fuzzy output using IF-THEN fuzzy rules and, finally, defuzzifier converts the fuzzy output into crisp values using membership functions.

The fuzzy logic system can also be visualized as an expert who based on certain rules, logics, and input information deduces solutions as outputs. The fuzzy rule system comprises a set of IF-THEN rules. For example, if a problem consists of three inputs x_1, x_2, x_3 and one output y, then the rules can be defined as follows.

Rule 1: if x_1 is $L1$ and x_2 is $M1$ and x_3 is $H1$, then y is $Y1$ else.

Rule 2: if x_1 is $L2$ and x_2 is $M2$ and x_3 is $H2$, then y is $Y2$ else.

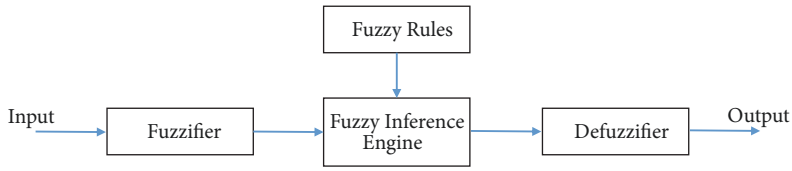

Figure 6: Various components of fuzzy system.

⋮

Rule n: if x_1 is Ln and x_2 is Mn and x_3 is Hn, then y is Yn.

where L_i, M_i, H_i, and Y_i are fuzzy subsets defined by the corresponding membership functions, i.e., μ_{Li}, μ_{Mi}, $\mu_{Hi,}$ and μ_{Yi}.

The execution of fuzzy logic in this work was executed in the following manner. The Math Works MATLAB (R2018b), Fuzzy Logic Toolbox was utilized to develop the fuzzy logic inference system. Consequently, the decision regarding the selection of the type of the fuzzy tool box was made. There were two types of fuzzy inference systems, including Mamdani type and Sugeno type that could be utilized in Fuzzy Logic Toolbox. However, Mamdani's fuzzy inference method was preferred because it is an intuitive based approach, possesses a widespread acceptance, and involves human input rather than mathematical analysis and it was easy to use for the problem presented in this work. Note that the output of IF-THEN rules in Mamdani systems is a fuzzy set rather than a constant or linear function.

The decisions regarding the number of membership functions (MFs), their shapes (or functional forms), and intervals are also significant in the design of a fuzzy logic system. As yet, there have been fewer substantial works in the literature which can demonstrate the predominance of a particular MF. Nevertheless, Zhao and Bose [40] evaluated the performance of different types of MFs in the fuzzy speed control of a vector-controlled induction motor drive. Their results established the superior performance of the triangular MF (trimf) as well as confirmed that the trapezoidal MF (trapmf) response was very close to that of triangular MF. It was also concluded that their results can also be generalized to other types of system. Additionally, these MFs adapt appropriately to the interpretation of any concept and they are easy to characterize, straightforward to represent, and are computationally simple. Therefore, the triangular and trapezoidal shaped MFs were chosen depending on the literature, knowledge, and experience elicited from the experts due to their simplicity and ease of application. Subsequent to the selection of the shapes of MFs, the decision regarding their number had to be made. It was very crucial to choose a proper number of MFs depending on the nature of the problem. It can be attributed to the fact that a sharpened judgement can be attained with a larger number of MFs, while a lower computational complexity is involved with a smaller number of MFs [41, 42]. Henceforth, in this work, the number of fuzzy subsets was decided depending on the expert opinion and the data gathered through experiments.

The development of fuzzy systems can be difficult, when it comes to determining the appropriate intervals for MFs. The overlapping fuzzy subsets have been considered as one of the greatest strengths because it provides robustness and stability to the fuzzy logic system [41]. A suitable overlapping was critical between different fuzzy sets in order to achieve a satisfactory completeness. The completeness level, which can assure the convergence of control as well as a lower overshoot, should be adopted [43]. In this work, the approach based on the experts' insights and knowledge of the application domain was adopted to specify the intervals. In a fuzzy rule based system, fuzzy rules constitute an important mechanism for characterizing different forms of knowledge as well as modeling the interactions between different variables [44]. As a result, sixteen fuzzy rules were established through extensive literature survey as well as the knowledge and experience elicited from the experts. Finally, a defuzzification method known as centroid approach was employed to translate the fuzzy output into a nonfuzzy value. The nonfuzzy value provided Performance Index (PI), where the larger PI indicated a better performance characteristic.

2.5. Validation. The confirmation experiment run was executed in order to analyze the utilization of the scanning probe at the selected scanning parameters. The acquired performance was compared with the predicted values and the results attained at the randomly selected scanning parameters. The PI (and *GRG*), using the optimal level of the scanning parameters, was predicted from following equation [45].

$$P = P_A + \sum_{i=1}^{m} \left(P_O - P_A\right) \tag{10}$$

where P_A is the total average of the PI (or the total mean of *GRG*), P_O is the average PI (or average *GRG*) at optimal level, and m is the number of scanning parameters that affect the performance characteristics.

3. Analysis

The main effect plot and Pareto chart for the scanning time are shown in Figure 7. It shows that the effect of all the scanning parameters is significant and different as depicted in Figure 7(a). In this main effects plot, it appears that scanning speed 10 mm/s, distance between points 0.01 mm, and the distance between lines 0.7 mm are associated with the lowest scanning time. The Pareto charts, which represent the absolute values of the standardized effects, were used to arrange the scanning parameters in the decreasing order of

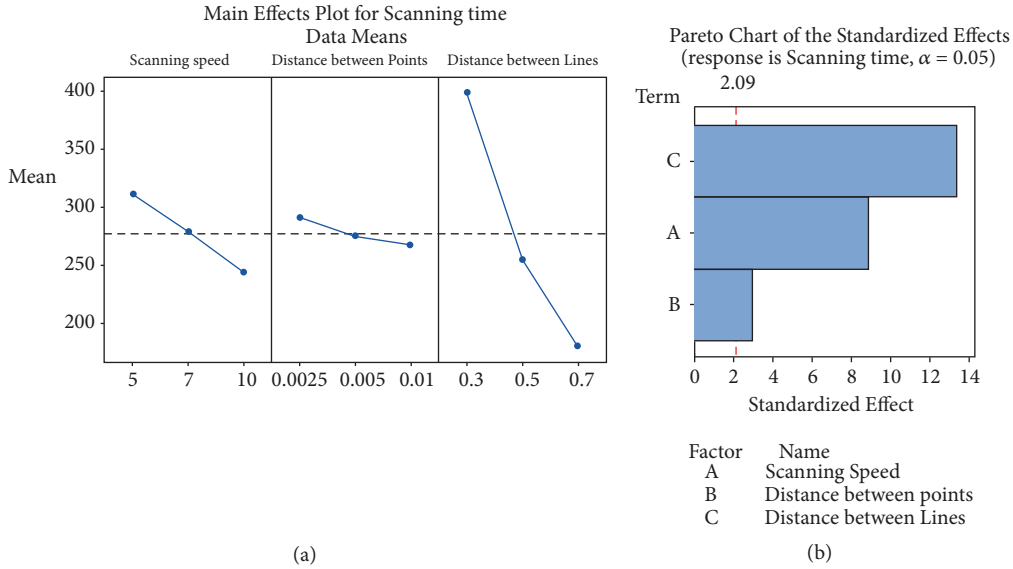

Figure 7: Plots for scanning time: (a) main effect; (b) Pareto chart.

their importance. As shown in Figure 7(b), it can be realized that the distance between lines had the largest effect on the scanning time, followed by the scanning speed and the distance between points.

The main effect plot and Pareto chart for the RMS are shown in Figure 8. As seen in Figure 8(a), it emerges that scanning speed 5 mm/s, distance between points 0.0025 mm, and distance between lines 0.3 mm are related to the lowest RMS. In Figure 8(b), it is shown that the scanning speed had the largest effect on the RMS, followed by the distance between lines and the distance between points.

These outcomes provide some useful information such as the contribution of various scanning parameters on different responses. It is clear that the scanning time decreases at higher distance between lines, higher distance between points, and a faster scanning speed. However, the RMS is increased (or the accuracy is reduced) at the higher values of these parameters. It necessitates the need of an appropriate combination of scanning parameters which can maintain a befitting balance between scanning time and the desired accuracy. It is axiomatic and self-evident that the scanning time is inversely proportional to distance between lines, scanning speed, and distance between points. In contrast, the RMS has shown a direct relationship with the scanning factors. At a higher scanning speed, the effect of dynamic forces also raises owing to a continuously changing velocity direction in scanning probes. It increases the measurement uncertainty and hence results in the reduction in accuracy. Additionally, a slower measurement speed is crucial to minimize deflection of the CMM's structure induced by acceleration and deceleration during the scanning process. Similarly, the values for distance between lines and distance between points should be kept at lower values for smaller RMS. It can be attributed to the fact that their larger values often result in overlooking indistinct changes in surface direction and fluctuations in the specimen surface quality. It can also be mentioned that the lower values of distance between points are also important in order to phase out the influence of vibration produced during the movement by scanning probe along the workpiece. Moreover, the distance between lines should not be kept very small because the unduly short distance may not provide sufficient time for the probe undulation to mitigate or stabilize before the subsequent scan line.

The analysis of individual single responses as noticed from the main effect plots provided in the foregoing paragraphs suggests that an eventual decision on the optimized scanning parameter setting cannot be achieved at this moment. It is because the influence of the parameters and their contributions to each response is very different. Accordingly, multiresponse optimization becomes essential. Therefore, the response data as given in Table 3 were methodically prepared to analyze multiresponse characteristics. The two measured responses, namely, scanning time and RMS, were utilized as input to GRA-PCA and fuzzy logic system for attaining the best combinations of scanning parameters.

The FFD based GRA, multiperformance optimization of coordinate metrology enhanced the scanning performance in terms of scanning time and RMS. The conversion of incomparable data into a comparable sequence in the range between zero and unity was performed using (2). For example, the comparability sequence for the experiment run 1 with response values of 270.96 min and 21 μm was achieved as follows.

Scanning time = (471.98 – 270.96)/(471.96-153.23) (maximum = 471.98 & minimum = 153.23)

Scanning time = 201.02/318.75

Scanning time = 0.6307

RMS = (38 – 21)/(38-15) (maximum = 38 & minimum = 15)

RMS = 17/23

RMS = 0.7391

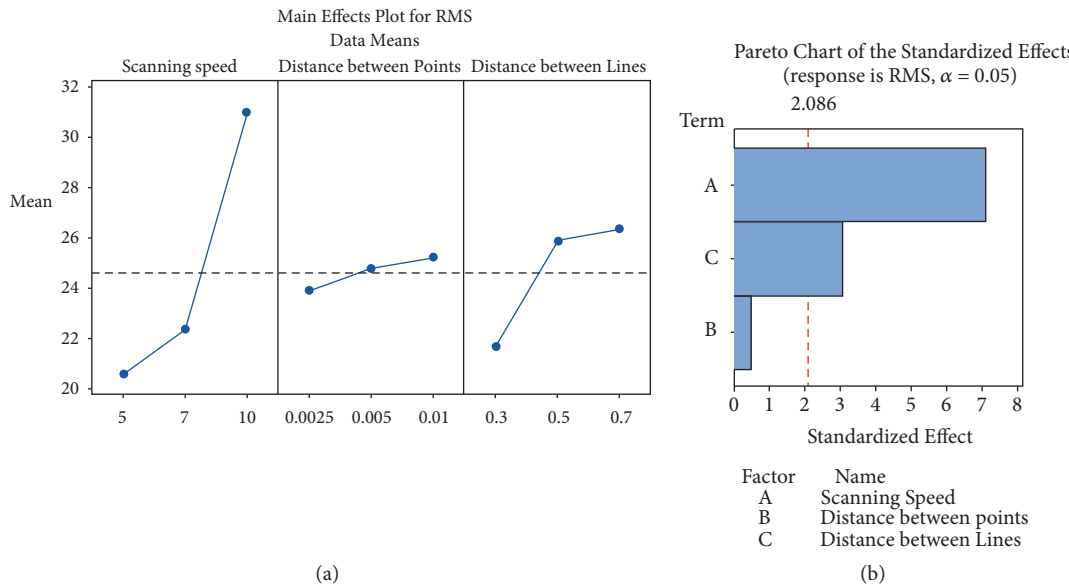

Figure 8: Plots for RMS: (a) main effect; (b) Pareto chart.

Thus, the comparability sequence obtained for the experiment run 1 was (0.6307, 0.7391). Similarly, the comparability sequences for the remaining experiment runs were estimated as presented in Table 4(a). Further, the reference sequence was identified by pursuing the maximum value from the comparability sequence of the scanning time and the RMS.

Reference Sequence =(Scanning time, RMS) = (1, 1)

The comparability sequences were further processed into the *GRC*s using (4) and (5) as follows. Therefore, the deviation sequence of scanning time and RMS for the experimental run 1 was determined as follows.

$\Delta_{o1}\ (1) = 1 - 0.6307$

$\Delta_{o1}\ (1) = 0.3693$

$\Delta_{o2}\ (1) = 1 - 0.7391$

$\Delta_{o2}\ (1) = 0.2609$

Finally, the deviation sequence determined for the experimental run 1 was (0.3693, 0.2609). Likewise, the deviation sequences for the residual experiment runs were computed, which are shown in Table 4(b). Next, the *GRC*s were determined for all the experiment runs and they are depicted in Table 4(c). The *GRC* calculation steps, considering the experiment run 1, can be described as follows.

For scanning time,

$GRC = (0 + 0.5 * 1)/(0.3693 + 0.5 * 1)$ ($\Delta_{\min} = 0$; $\Delta_{\max} = 1$; $\epsilon = 0.5$)

$GRC = 0.5751$

For RMS,

$GRC = (0 + 0.5 * 1)/(0.2609 + 0.5 * 1)$ ($\Delta_{\min} = 0$; $\Delta_{\max} = 1$; $\epsilon = 0.5$)

$GRC = 0.6571$

The *PCA* was performed in order to find out the weighting values to be multiplied with the *GRC*s (Table 4(c)) for each response parameter. The *GRC* data were utilized to obtain *CCA* using (6).

$$CCA = \begin{bmatrix} 1 & -0.5898 \\ -0.5898 & 1 \end{bmatrix} \tag{11}$$

The *CCA* was further processed to find out eigenvalues and eigenvectors using (7). The eigenvector that corresponded to the largest eigenvalue 1.5898 was [-0.7071, 0.7071] as shown in Table 5.

The square of the elements of the first principal component provided a weighting to the *GRC*s of the corresponding response variable. The weightings or contributions of each response parameter to the optimization problem so obtained are given in Table 6.

Finally, the weighting was multiplied with the respective *GRC*s of each experiment run using (9). As a result, the two *GRC*s were combined into a *GRG* as shown in Table 7. It is clear that the experiment run 23 resulted in largest value of *GRG*.

The level-wise mean of the *GRG* for each scanning parameter was also estimated and is shown in Table 8. It was computed by taking the average of those values of *GRG* with the same levels of every scanning parameter. In this way, the average *GRG*s for scanning speed at Level-1, scanning speed at Level-2, scanning speed at Level-3, distance between points at Level-1, distance between points at Level-2, and so on were estimated.

Evidently, the larger the value of *GRG*, the better the multiple-response parameter. Based on Table 7 and according to response table (Table 8), Level 2, Level 1, and Level 3 provide the largest values of *GRG* for scanning speed, distance between points, and the distance between lines, respectively. Therefore, Level 2, Level 1, and Level 3 are the condition for

Table 4: (a) Comparability sequences; (b) deviation sequences; (c) *GRC*s.

(a)

Comparability Sequences	
Scanning time	RMS
0.6307	0.7391
0.8286	0.6522
0.3426	0.5652
0.2113	0.8261
0.9475	0.6522
0.9535	0.1304
0.3581	0.5652
0.8436	0.3043
0.8131	0.7826
0.9714	0.2174
0.2578	0.6087
0.6869	0.7391
0.6593	0.6957
0.2242	0.6522
1.0000	0.3478
0.8107	0.0000
0.1393	0.9130
0.8426	0.5652
0.4841	0.7391
0.5717	0.7391
0.6467	0.6957
0.1703	0.7391
0.9334	0.7391
0.9785	0.4783
0.0000	1.0000
0.8126	0.0870
0.3612	0.5217
Reference sequence	
1	1

(b)

Deviation Sequences	
Scanning time	RMS
0.3693	0.2609
0.1714	0.3478
0.6574	0.4348
0.7887	0.1739
0.0525	0.3478
0.0465	0.8696
0.6419	0.4348
0.1564	0.6957
0.1869	0.2174
0.0286	0.7826
0.7422	0.3913
0.3131	0.2609

(b) Continued.

Deviation Sequences	
Scanning time	RMS
0.3407	0.3043
0.7758	0.3478
0.0000	0.6522
0.1893	1.0000
0.8607	0.0870
0.1574	0.4348
0.5159	0.2609
0.4283	0.2609
0.3533	0.3043
0.8297	0.2609
0.0666	0.2609
0.0215	0.5217
1.0000	0.0000
0.1874	0.9130
0.6388	0.4783

(c)

*GRC*s	
Scanning time	RMS
0.5751	0.6571
0.7447	0.5897
0.4320	0.5349
0.3880	0.7419
0.9050	0.5897
0.9149	0.3651
0.4379	0.5349
0.7617	0.4182
0.7279	0.6970
0.9459	0.3898
0.4025	0.5610
0.6149	0.6571
0.5948	0.6216
0.3919	0.5897
1.0000	0.4340
0.7254	0.3333
0.3675	0.8519
0.7606	0.5349
0.4922	0.6571
0.5386	0.6571
0.5860	0.6216
0.3760	0.6571
0.8824	0.6571
0.9588	0.4894
0.3333	1.0000
0.7274	0.3538
0.4391	0.5111

Table 5: Eigenvalues and eigenvectors for principal components.

	Eigenvalue	Eigenvector	
		Scanning time	RMS
First Principal Component	1.5898	-0.7071	0.7071
Second Principal Component	0.4102	-0.7071	-0.7071

Table 6: Weightage and contribution of individual response.

Response	Weight	Contribution (%)
Scanning time	0.50	50
RMS	0.50	50

the optimal parameter combination of the scanning using a scanning touch probe, i.e., scanning speed at 7 mm/s, distance between points at 0.0025 mm, and the distance between lines at 0.7 mm. The mean of the *GRG* plot shown in Figure 9 also clearly represents the response of the scanning parameters on *GRG*. The level-wise *GRG* plot also depicts the variation in the multiresponse when the scanning parameters change between different levels. When the values of the last column in Table 8 are compared, it is evident that the difference between the maximum and minimum values of *GRG* for distance between lines is the largest, followed by scanning speed and distance between points. This specifies that the distance between lines has the strongest effect on the multiresponse parameter, followed by scanning speed and distance between points.

The fuzzy logic was also implemented in order to ascertain the results acquired using GRA-PCA. Four fuzzy subsets (Low, Medium, High, and Very High) were assigned to the two inputs, scanning time and RMS as shown in Figures 10(a) and 10(b), respectively. Six fuzzy subsets were designated to the output (PI) as depicted in Figure 10(c).

The different intervals as shown in Table 9 were chosen for various MFs in order to better describe the process of data acquisition as well as optimize the scanning parameters.

Additionally, sixteen fuzzy rules were established depending on the fact that a lower scanning time and lower RMS provided better performance, i.e., higher PI. The assigned fuzzy rule base consisted of IF-THEN control rules with two inputs and one output. The different rules were as follows:

(i) If (Scanning_time is Low) and (RMS is Low) Then (Productivity is Best)

(ii) If (Scanning_time is Medium) and (RMS is Medium) Then (Productivity is High)

(iii) If (Scanning_time is High) and (RMS is High) Then (Productivity is Very Low)

(iv) If (Scanning_time is Very High) and (RMS is Very High) Then (Productivity is Worst)

(v) If (Scanning_time is Low) and (RMS is Medium) Then (Productivity is Very High)

(vi) If (Scanning_time is Low) and (RMS is High) Then (Productivity is High)

(vii) If (Scanning_time is Low) and (RMS is Very High) Then (Productivity is Low)

(viii) If (Scanning_time is Medium) and (RMS is Low) Then (Productivity is High)

(ix) If (Scanning_time is Medium) and (RMS is High) Then (Productivity is Low)

(x) If (Scanning_time is Medium) and (RMS is Very High) Then (Productivity is Very Low)

(xi) If (Scanning_time is High) and (RMS is Low) Then (Productivity is High)

(xii) If (Scanning_time is High) and (RMS is Medium) Then (Productivity is Low)

(xiii) If (Scanning_time is High) and (RMS is Very High) Then (Productivity is Very Low)

(xiv) If (Scanning_time is Very High) and (RMS is Low) Then (Productivity is Low)

(xv) If (Scanning_time is Very High) and (RMS is Medium) Then (Productivity is Very Low)

(xvi) If (Scanning_time is Very High) and (RMS is High) Then (Productivity is Very Low)

After the execution of the fuzzy logic, the PI for various experiment runs was determined. Table 10 represents the outcomes of the PI for different experiment runs.

In order to differentiate the influence of each scanning parameter on the PI at different levels, the average of PI was computed. For example, the average of PI for scanning speed at Level 1 can be calculated by numerical mean of PI values for the experiments 1, 2, 9, 17, 18, 19, 21, 22, and 25. Similarly, the average of PI for each level of other scanning parameters was estimated. The average PI at each level for the different scanning parameters is shown in Table 11.

The effect of various scanning parameters can also be precisely represented through PI response graphs. The PI graphs depict the variation in the response when a particular factor changes from Level 1 to Level 3. Based on the response graph (Figure 11) and response table (Table 11), the optimal scanning parameters for coordinate measurement can be acquired. Generally, the larger the PI, the better the performance characteristics. It was observed from experimental results that the combination for experiment number 23 had the highest PI, as presented in Table 10. Therefore, depending on Table 10 and response table (Table 11), Level 2, Level 1, and Level 3 provide the largest values of PI for scanning speed, distance between points, and the distance between lines, respectively. Hence, Level 2 (7 mm/s), Level 1 (0.0025 mm),

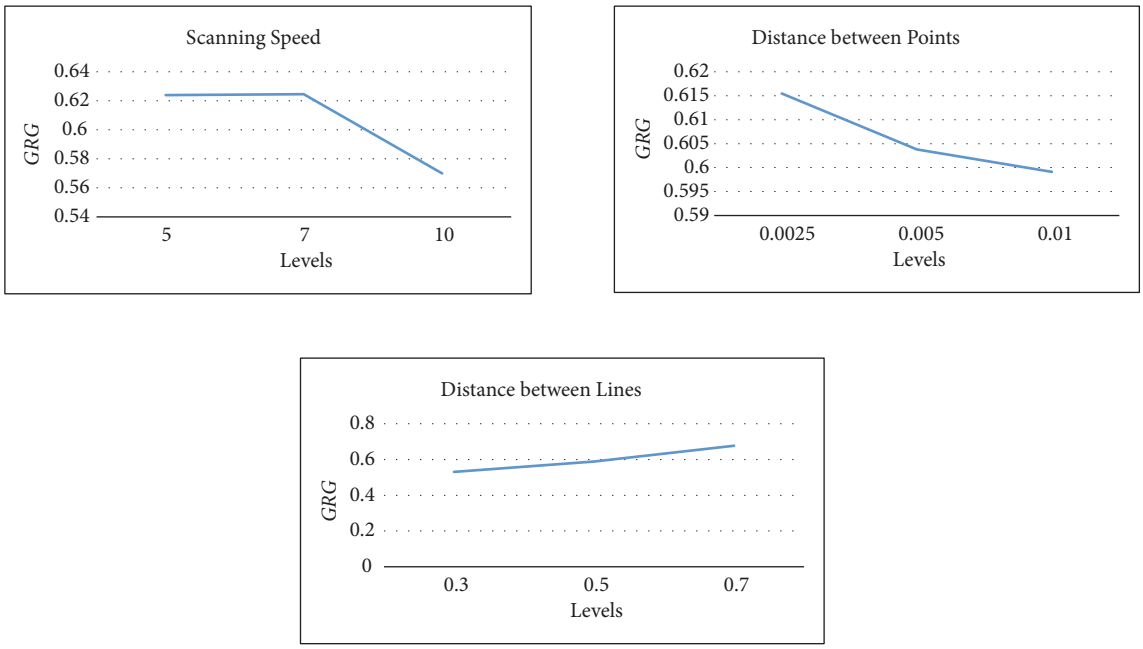

Figure 9: *GRG* response graphs.

Table 7: *GRG* and ranking of different experiment runs.

Experiment Run	*GRG*	Order	Experiment Run	*GRG*	Order	Experiment Run	*GRG*	Order
1	0.6161	12	10	0.6679	6	19	0.5747	18
2	0.6672	7	11	0.4817	26	20	0.5979	16
3	0.4834	25	12	0.6360	11	21	0.6038	15
4	0.5650	19	13	0.6082	14	22	0.5166	22
5	0.7474	2	14	0.4908	23	23	0.7698	1
6	0.6400	10	15	0.7170	4	24	0.7241	3
7	0.4864	24	16	0.5294	21	25	0.6667	8
8	0.5899	17	17	0.6097	13	26	0.5406	20
9	0.7124	5	18	0.6477	9	27	0.4751	27

Table 8: Average *GRG* at different levels.

Scanning Parameter	*GRG*			
	Level 1	Level 2	Level 3	Max-Min
Scanning speed	0.6239	0.6245	0.5700	0.0546
Distance between points	0.6155	0.6038	0.5991	0.0164
Distance between lines	0.5306	0.5885	0.6769	0.1463
Total average of *GRG*		0.6036		

and Level 3 are the settings to aptly utilize a scanning touch probe.

It can also be established from the last column in Table 11 that the distance between lines had the strongest effect on the multiresponse control, followed by scanning speed and distance between points.

Table 12 shows the comparisons of CMM performance mounted with a scanning touch probe at the optimized and the initial parameter settings. The experimental outcome at the optimized settings was also analyzed with respect to the predicted performance. The utilization of the scanning probe using PI (and *GRG*) at the optimal settings was predicted using (10), as follows.

$$P_A = 0.2981;\ m = 3$$

$$\sum_{i=1}^{m}(P_O - P_A) = (0.3299\text{-}0.2981) + (0.3141\text{-}0.2981) + (0.3483\text{-}0.2981) = 0.1043$$

$$P = 0.2981 + 0.098 = 0.3961$$

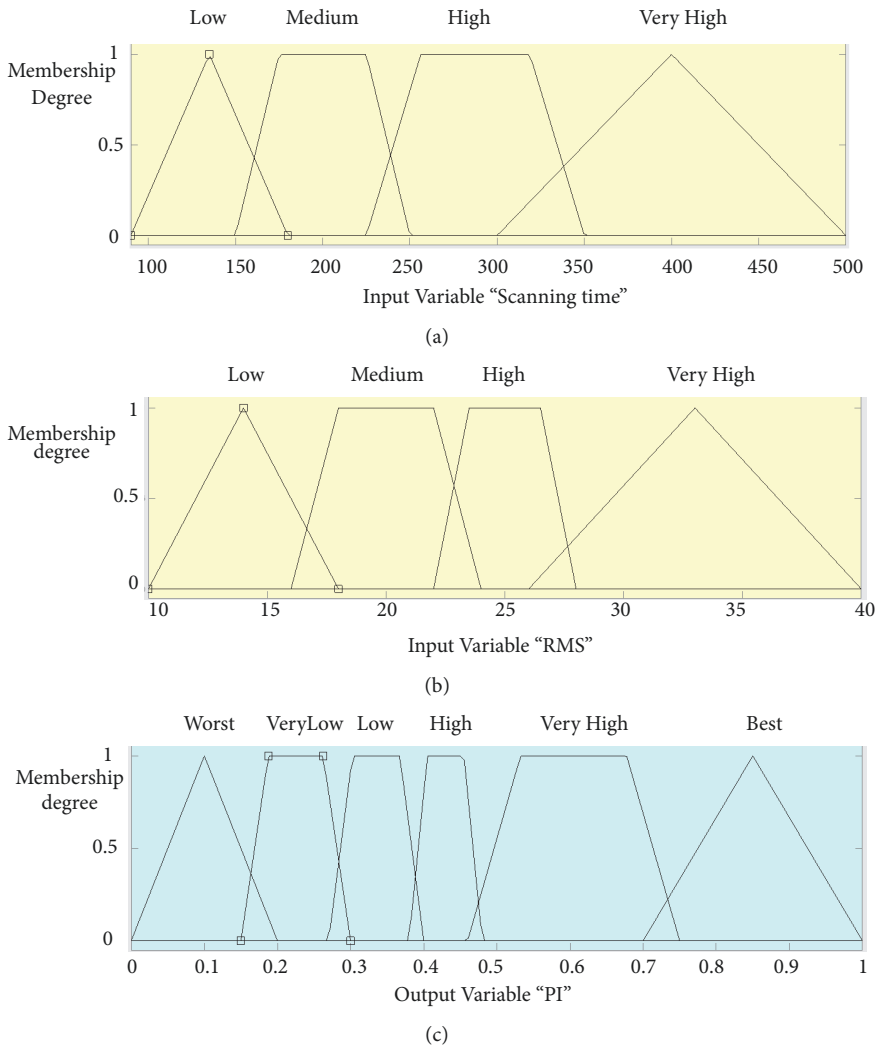

Figure 10: Membership plots: (a) scanning time; (b) RMS; output variable (PI).

Table 9: Definition of input and output variables.

Variable		Type of membership function	Levels	Interval
Input	Scanning time Range (90-500)	trimf	Low	< 180
		trapmf	Medium	150-250
		trapmf	High	225-350
		trimf	Very High	> 300
	RMS Range (10-40)	trimf	Low	< 18
		trapmf	Medium	16-24
		trapmf	High	22-28
		trimf	Very High	> 26
Output	PI Range (0-1)	trimf	Worst	< 0.20
		trapmf	Very Low	0.15-0.30
		trapmf	Low	0.27-0.40
		trapmf	High	0.38-0.48
		trapmf	Very High	0.46-0.75
		trimf	Best	> 0.70

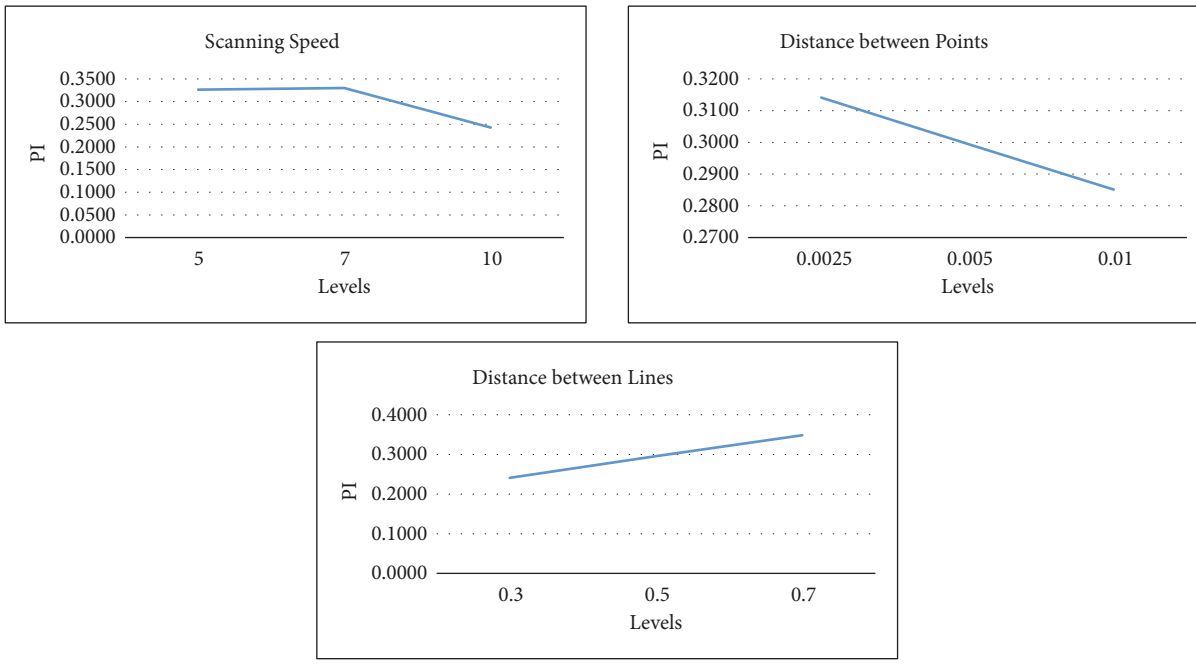

Figure 11: PI response graphs.

Table 10: Outcomes of PI.

Experiment Run	PI	Experiment Run	PI	Experiment Run	PI
1	0.335	10	0.270	19	0.313
2	0.370	11	0.225	20	0.335
3	0.225	12	0.335	21	0.335
4	0.225	13	0.335	22	0.225
5	0.453	14	0.225	23	0.486
6	0.253	15	0.311	24	0.350
7	0.225	16	0.225	25	0.335
8	0.225	17	0.258	26	0.225
9	0.430	18	0.335	27	0.225

Table 11: Mean PI at various levels.

Scanning Parameter	PI			
	Level 1	Level 2	Level 3	Max-Min
Scanning Speed	0.3262	0.3299	0.2427	0.0872
Distance between Points	0.3141	0.2996	0.2851	0.0290
Distance between Lines	0.2409	0.2959	0.3483	0.1074
Total average of PI		0.2981		

The outcomes from the validation step as shown in Table 12 implies that the scanning parameters established using GRA-PCA and fuzzy logic are robust and stable. Henceforth, the final optimal scanning settings are scanning time 7 mm/s, distance between points 0.0025 mm, and the distance between lines 0.7 mm.

4. Conclusion

The appropriate combination of scanning parameters is essential in scanning touch probe in order to optimize its scanning performance. The presence of different measurement uncertainties in coordinate metrology advocates the techniques, which assume vagueness and ambiguity in the data. Therefore, this article has established a methodology using the Grey–PCA and fuzzy logic for optimizing multiple attributes (scanning time and accuracy) to enhance the quality of the digitization. This work has explained the execution of GRA-PCA and fuzzy logic in optimizing the scanning performance of the CMM. The two techniques provided the combination of scanning speed (7 mm/s), distance between points (0.0025 mm), and the distance between lines (0.7 mm)

Table 12: Outcomes using the random and optimal scanning parameters.

Technique	GRA			Fuzzy Logic		
	Random Scanning Parameters	Predicted	Experimental	Random Scanning Parameters	Predicted	Experimental
Combination	Scanning Speed - 10 Distance between Points - 0.01 Distance between Lines - 0.3	0.7097	Scanning Speed - 7 Distance between Points - 0.0025 Distance between Lines - 0.7	Scanning Speed - 10 Distance between Points - 0.01 Distance between Lines - 0.3	0.3961	Scanning Speed - 7 Distance between Points - 0.0025 Distance between Lines - 0.7
GRG/PI	0.4751		0.7823	0.2250		0.4600
	Improvement in *GRG*	0.3072		Improvement in PI	0.2350	

as the most suitable scanning setting. Indeed, the outcomes from the two approaches corroborates with each other, thus substantiating their application in coordinate measurement. The two techniques certainly streamlined the optimization of scanning procedure with multiple responses. Thus, the findings in this analysis can act as a guide for metrology experts and CMM engineers or operators who require determining the optimal result of scanning conditions.

The outcomes in this study provide helpful instructions pertaining to the influence of scanning parameters on scanning time and RMS. For example, the scanning time was inversely proportional to the distance between lines, scanning speed, and distance between points. Similarly, the RMS had a direct correspondence with the scanning parameters. It can be inferred that the dynamic effects are significant, especially in CMMs mounted scanning probes. It can be attributed to the fact that the scanning is frequently carried out along a curved path or free form surfaces, causing the CMM to regularly accelerate or decelerate and alter directions while probing coordinates. Certainly, these dynamic effects contribute significantly to the measurement uncertainties during the data acquisition by scanning probes. This necessitates the need of a lower scanning speed, which can reduce the variation in CMM's structure emanating from inconsistent speeds during digitization. Moreover, the higher values of the distance between points and the distance between lines should not be favored as they repeatedly ignore small, but consequential variations in surface conditions. The lower values of distance between points are also crucial to overcome the effect of vibrations during measurement with scanning probes.

This research is distinctive owing to its intelligent optimization methods, incorporating uncertainties and improving the performance of scanning probes. The utilized optimization methods are user-friendly, simple, and assist in rational, efficient, and feasible decision making. Since the parameters in this work have been determined by considering the measurement uncertainty, it can be stated that the outcomes from this study are robust and adequate. The utilization of GRA-PCA and fuzzy logic made the selection of scanning parameters reliable and more realistic. These methods are of particular interest in processes such as scanning, which involve significant uncertainties from various sources. Nevertheless, these optimization approaches can become exhausting, computationally expensive, and time-taking, with an increase in the number of influencing factors and the responses. As the selection of factors in scanning probes has not been dealt with methodically and adequately due to its complex nature, this work intends to aid CMM users to optimize the scanning performance. Obviously, the outcome of this investigation can be applied to other probing systems and can be extended to include more experiments and parameters in various situations as required by the specific application.

Data Availability

All the data is included within the manuscript itself.

Conflicts of Interest

The authors declare that they have no conflicts of interest.

Acknowledgments

The authors extend their appreciation to the Deanship of Scientific Research at King Saud University for funding this work through research group number RG-1440-026.

References

[1] R. G. Wilhelm, R. Hocken, and H. Schwenke, "Task specific uncertainty in coordinate measurement," *CIRP Annals - Manufacturing Technology*, vol. 50, no. 2, pp. 553–563, 2001.

[2] K. Takamasu, "Present problems in coordinate metrology for nano and micro scale measurements," *MAPAN*, vol. 26, no. 1, pp. 3–14, 2011.

[3] E. Savio, L. De Chiffre, and R. Schmitt, "Metrology of freeform shaped parts," *CIRP Annals - Manufacturing Technology*, vol. 56, no. 2, pp. 810–835, 2007.

[4] E. Vezzetti, "Reverse engineering: A selective sampling acquisition approach," *The International Journal of Advanced Manufacturing Technology*, vol. 33, no. 5-6, pp. 521–529, 2007.

[5] P. Pereira and R. Hocken, "Characterization and compensation of dynamic errors of a scanning coordinate measuring machine," *Precision Engineering*, vol. 31, no. 1, pp. 22–32, 2007.

[6] C. Feng and V. Pandey, "Experimental study of the effect of digitizing parameters on digitizing uncertainty with a CMM," *International Journal of Production Research*, vol. 40, no. 3, pp. 683–697, 2002.

[7] A. Piratelli-Filho and B. Di Giacomo, "CMM uncertainty analysis with factorial design," *Precision Engineering*, vol. 27, no. 3, pp. 283–288, 2003.

[8] C. J. Feng, A. L. Saal, J. G. Salsbury, A. R. Ness, and G. C. Lin, "Design and analysis of experiments in CMM measurement uncertainty study," *Precision Engineering*, vol. 31, no. 2, pp. 94–101, 2007.

[9] M. Korosec, J. Duhovnik, and N. Vukasinovic, "Process modelling of non-contact reverse engineering process," in *Proceedings of the 7th WSEAS International Conference on Signal Processing, Computational Geometry & Artificial Vision*, Athens, Greece, 2007.

[10] V. K. Pathak and A. K. Singh, "Optimization of morphological process parameters in contactless laser scanning system using modified particle swarm algorithm," *Measurement*, vol. 109, pp. 27–35, 2017.

[11] N. Tosun, "Determination of optimum parameters for multi-performance characteristics in drilling by using grey relational analysis," *The International Journal of Advanced Manufacturing Technology*, vol. 28, no. 5-6, pp. 450–455, 2006.

[12] A. N. Siddiquee, Z. A. Khan, and Z. Mallick, "Grey relational analysis coupled with principal component analysis for optimisation design of the process parameters in in-feed centreless cylindrical grinding," *The International Journal of Advanced Manufacturing Technology*, vol. 46, no. 9–12, pp. 983–992, 2010.

[13] A. Taşkesen and K. Kütükde, "Experimental investigation and multi-objective analysis on drilling of boron carbide reinforced metal matrix composites using grey relational analysis," *Measurement*, vol. 47, no. 1, pp. 321–330, 2014.

[14] H. S. Lu, C. K. Chang, N. C. Hwang, and C. T. Chung, "Grey relational analysis coupled with principal component analysis for optimization design of the cutting parameters in high-speed end milling," *Journal of Materials Processing Technology*, vol. 209, no. 8, pp. 3808–3817, 2009.

[15] A. K. Sehgal and Meenu, "Grey relational analysis coupled with principal component analysis to optimize the machining process of ductile iron," *Materials Today: Proceedings*, vol. 5, no. 1, pp. 1518–1529, 2018.

[16] C.-J. Tzeng, Y.-H. Lin, Y.-K. Yang, and M.-C. Jeng, "Optimization of turning operations with multiple performance characteristics using the Taguchi method and Grey relational analysis," *Journal of Materials Processing Technology*, vol. 209, no. 6, pp. 2753–2759, 2009.

[17] R. Ramanujam, K. Venkatesan, V. Saxena, R. Pandey, T. Harsha, and G. Kumar, "Optimization of machining parameters using fuzzy based principal component analysis during dry turning operation of inconel 625 - A hybrid approach," *Procedia Engineering*, vol. 97, pp. 668–676, 2014.

[18] J. L. Mercy, S. Prakash, A. Krishnamoorthy, S. Ramesh, and D. Alex Anand, "Multi response optimisation of mechanical properties in self-healing glass fiber reinforced plastic using grey relational analysis," *Measurement*, vol. 110, pp. 344–355, 2017.

[19] C. L. Lin, J. L. Lin, and T. C. Ko, "Optimisation of the EDM process based on the orthogonal array with fuzzy logic and grey relational analysis method," *The International Journal of Advanced Manufacturing Technology*, vol. 19, no. 4, pp. 271–277, 2002.

[20] G. Liu, C. Li, Y. Zhang et al., "Process parameter optimization and experimental evaluation for nanofluid MQL in grinding Ti-6Al-4V based on grey relational analysis," *Materials and Manufacturing Processes*, vol. 33, no. 9, pp. 950–963, 2017.

[21] C. B. Maheswaran, R. Jayendra Bharathi, S. Paul Joshua, and A. Kumar Srirangan, "Optimization of laser welding parameters for incoloy 800HT joints using Grey-fuzzy Taguchi approach," *Materials Today: Proceedings*, vol. 5, pp. 14237–14243, 2018.

[22] Y. Zhang, C. Li, D. Jia, D. Zhang, and X. Zhang, "Experimental evaluation of MoS2 nanoparticles in jet MQL grinding with different types of vegetable oil as base oil," *Journal of Cleaner Production*, vol. 87, pp. 930–940, 2015.

[23] Y. Wang, C. Li, Y. Zhang et al., "Experimental evaluation of the lubrication properties of the wheel/workpiece interface in MQL grinding with different nanofluids," *Tribology International*, vol. 99, pp. 198–210, 2016.

[24] D. Jia, C. Li, Y. Zhang et al., "Experimental evaluation of surface topographies of NMQL grinding ZrO2 ceramics combining multiangle ultrasonic vibration," *The International Journal of Advanced Manufacturing Technology*, vol. 100, no. 1-4, pp. 457–473, 2019.

[25] J. Antony, *Full Factorial Designs, Design of Experiments for Engineers and Scientists*, Chapter 6, Elsevier, 2nd edition, 2014.

[26] B. Jones and D. Montgomery, "Design of experiments- partial replication of small factorial designs," *Statistics Digest - The Newsletter of the ASQ Statistics Division*, vol. 36, no. 3, pp. 17–22, 2017.

[27] S. Cheng, J. Miao, and S. Wu, "Investigating the effects of operational factors on PEMFC performance based on CFD simulations using a three-level full-factorial design," *Journal of Renewable Energy*, vol. 39, no. 1, pp. 250–260, 2012.

[28] S. H. Mian, M. Mannan, and A. Al-Ahmari, "Accuracy of a reverse-engineered mould using contact and non-contact measurement techniques," *International Journal of Computer Integrated Manufacturing*, vol. 28, no. 5, pp. 419–436, 2014.

[29] K. Palanikumar, B. Latha, V. S. Senthilkumar, and J. P. Davim, "Analysis on drilling of glass fiber-reinforced polymer (GFRP) composites using grey relational analysis," *Materials and Manufacturing Processes*, vol. 27, no. 3, pp. 297–305, 2012.

[30] D. Ju-Long, "Control problems of grey systems," *Systems & Control Letters*, vol. 1, no. 5, pp. 288–294, 1982.

[31] A. Malek, S. Ebrahimnejad, and R. Tavakkoli-Moghaddam, "An improved hybrid grey relational analysis approach for green resilient supply chain network assessment," *Sustainability*, vol. 9, no. 8, article no. 1433, 2017.

[32] J. Hou, "Grey relational analysis method for multiple attribute decision making in intuitionistic fuzzy setting," *Journal of Convergence Information Technology*, vol. 5, no. 10, pp. 194–199, 2010.

[33] Z.-C. Lin and C.-Y. Ho, "Analysis and application of grey relation and ANOVA in chemicalmechanical polishing process parameters," *The International Journal of Advanced Manufacturing Technology*, vol. 21, no. 1, pp. 10–14, 2003.

[34] M. H. Abidi, A. M. Al-Ahmari, A. N. Siddiquee, S. H. Mian, M. K. Mohammed, and M. S. Rasheed, "An investigation of the micro-electrical discharge machining of nickel-titanium shape memory alloy using grey relations coupled with principal component analysis," *Metals*, vol. 7, no. 11, pp. 1–15, 2017.

[35] K. Pearson, "On lines and planes of closest fit to systems of points in space," *Philosophical Magazine*, vol. 2, pp. 559–572, 1901.

[36] H. Hotelling, "Analysis of a complex of statistical variables into principal components," *Journal of Educational Psychology*, vol. 24, no. 6, pp. 417–441, 1933.

[37] W.-S. Lee and Y.-C. Lin, "Evaluating and ranking energy performance of office buildings using Grey relational analysis," *Energy*, vol. 36, no. 5, pp. 2551–2556, 2011.

[38] L. A. Zadeh, "Fuzzy sets," *Information and Control*, vol. 8, no. 3, pp. 338–353, 1965.

[39] J. Ghose, V. Sharma, N. Kumar, A. Krishnamurthy, S. Kumar, and Z. Botak, "Taguchi-Fuzzy based mapping of EDM-machinability of aluminium foam," *Tehnički Vjesnik*, vol. 18, no. 4, pp. 595–600, 2011.

[40] J. Zhao and B. K. Bose, "Evaluation of membership functions for fuzzy logic controlled induction motor drive," in *Proceedings of the 28th Annual Conference of the IEEE Industrial Electronics Society (IECON '02)*, vol. 1, pp. 229–234, IEEE, Sevilla, Spain, November 2002.

[41] J. M. Mendel, "Fuzzy logic systems for engineering: a tutorial," *Proceedings of the IEEE*, vol. 83, no. 3, pp. 345–377, 1995.

[42] M. Mizumoto, "Fuzzy controls under various fuzzy reasoning methods," *Information Sciences*, vol. 45, no. 2, pp. 129–151, 1988.

[43] B. B. Meunier, M. Dotoli, and B. Maione, "On the choice of membership functions in a mamdani-type fuzzy controller," in *Proceedings of the First Online Workshop on Soft Computing*, Nagoya, Japan, 1996.

[44] L. Magdalena, "Fuzzy rule-based systems," in *Springer Handbook of Computational Intelligence. Springer Handbooks*, Kacprzyk J. and Pedrycz W., Eds., Springer, Berlin, Germany, 2015.

[45] K. Palanikumar, L. Karunamoorthy, R. Karthikeyan, and B. Latha, "Optimization of machining parameters in turning GFRP composites using a carbide (K10) tool based on the taguchi method with fuzzy logics," *Metals and Materials International*, vol. 12, no. 6, pp. 483–491, 2006.